



Proceedings of the Seventh International Conference on Charged Particle Optics

Possibilities for graphene for field emission: modeling studies using the BEM

S. Watcharotone^a, R. S. Ruoff^a, F. H. Read^{b*}

^a*Department of Mechanical Engineering, Northwestern University, Evanston, IL 60208, USA*

^b*School of Physics and Astronomy, University of Manchester, Manchester M13 9PL, UK*

Received 9 July 2008; received in revised form 9 July 2008; accepted 9 July 2008

Abstract

The Boundary Element Method has been used to model the field enhancement factors of free-standing sub-nanometre graphite sheets, which are thought to be suitable for use as field emission sources. The variation of the enhancement factor over the surfaces of the edges and corners of the rectangular sheets has been explored. The dependence of the enhancement factor on the thickness, height and width of the sheets has been found and the results have been parameterized where possible by simple empirical functions. © 2008 Elsevier B.V. All rights reserved.

PACS: 02.70.Pt; 79.70.+q

Keywords: Field emission; Graphene; Boundary element method

1. Introduction

Carbon nanotubes of various shapes and sizes have been used as field emission sources in several different devices, including flat-panel displays (for a recent review see Jonge and Bonard [1]). The current emitted by a nanotube depends on the field strength F_{tip} at its end, which is stronger than the applied macroscopic field F_m by a factor known as the ‘field enhancement factor’ β (sometimes called the field amplification factor and sometimes denoted by γ). That is,

$$\beta = F_{tip}/F_m \tag{1}$$

where F_{tip} is the maximum electrostatic field at the tip of the tube.

* Corresponding author. Tel.: +44-1625-425-759

E-mail address: frank.read@ieee.org

For a single isolated carbon nanotube the value of β depends on the length, radius and type of tube: this has been the subject of several experimental and computational investigations (e.g. Refs [2-11]). The dependence of β on the length and radius is now well understood for the type of closed-end tube known as a ‘hemisphere on a post’ in which the free end of the nanotube is a solid hemisphere that sits on a cylinder (which might be singly or multiply walled) which in turn sits perpendicularly on a flat plate. In practice nanotubes usually exist as arrays of tubes, which have also been investigated experimentally and computationally (e.g. Refs [12-17]).

Recently it has been suggested by Wang *et al* [18] that free-standing sub-nanometer ‘graphite’ sheets can be used as field emission sources. The purpose of the present study is to model the field enhancement factors of these sheets, using the Boundary Element Method (BEM). The BEM is ideal for calculating surface fields and is also ideal for treating very small structures in the presence of much larger electrodes. It has been used previously [11,17] to accurately model the field enhancement factors of various arrangements of carbon nanotubes, including single tubes, one- and two-dimensional arrays and random arrays. The CPO3D program [19] was used in these studies and is also used in the present study. The data files that have been used for the present study are freely available from the Web site. Each of these data files include a ‘comments’ section that gives further computational details that have not been included in the present paper.

2. Calculated field enhancement factors on the corners and edges of the graphite sheets

In the BEM the surfaces are subdivided into rectangular or triangular segments. In the present study the segments of the flat surfaces are rectangular and are made smallest near the edges and corners, using a subdivision technique that was previously used when calculating the capacitance of a cube [20,21]. The edges are assumed to have a rounded shape, with a semicircular section, and the corners are assumed to be spherical: the segments near a corner are shown in Fig. 1.

The initial simulation has been of a carbon sheet that has a height and width of 1 μm and a thickness of 1 nm. To create a field an anode is placed at an arbitrary 9 μm away, with a potential of 0.01 V, giving a nominal ‘far field’ of 1 V/mm.

To establish the field enhancement factor β it is necessary to find the fields at various points on the surface of the edge of the sheet. To achieve the highest accuracy the field at the surface is obtained by finding the field at a series of distances s from the surface and then fitting to the empirical function:

$$1/E(s) = a + b \cdot s + c \cdot s^2 \quad (2)$$

The field at the surface is then $E(0) = 1/a$. This choice of empirical function includes the extreme cases of the field near an isolated spherical corner, for which $b = 0$, the fields near an isolated cylindrical edge, for which $c = 0$, and the field near a flat surface, for which b and c are both zero.

We start by considering the behavior of β along a line that runs along the tops of the rounded edges and traverses the corner. The value of β on the center of the rounded edge is shown in Fig. 2 as a function of the distance from the central point of the corner. The highest value of β clearly occurs at the central point of the corner and is 384 for the present dimensions. This is 34% of the value [11,17] for an isolated nanotube that has the same end curvature and the same length as the height of the sheet. The value of β decreases quickly away from the corner and reaches the lowest value at the mid-point of the top edge, where it is 72 (which is off-scale in Fig. 2). In this region the sheet is essentially a 2-dimensional system since the field is only weakly dependent on the distance along the ridge: a lower value of β is therefore expected, compared with β at the 3-dimensional corners.

Next we consider how β varies away from the mid-point of the corner or rounded edge. Dealing firstly with the corner, it is useful to consider two vectors, the first from the point in question to the center of curvature of the corner and the second from the mid-point of the corner to the center of curvature. The angle θ is then the angle between these two vectors. Similarly for the edge we consider a vector from the point in question to the center of curvature of that section of the edge and a second vector from the nearest point at the middle of the rounded edge to the center of curvature. We then define ϕ as the angle between these two vectors. In other words ϕ is the angular displacement in the transverse direction.

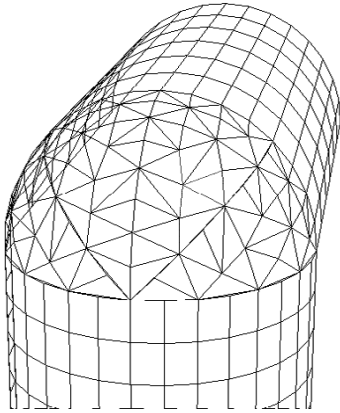


Fig. 1. Perspective 3D view of the segments near a corner of a ‘graphite’ sheet.

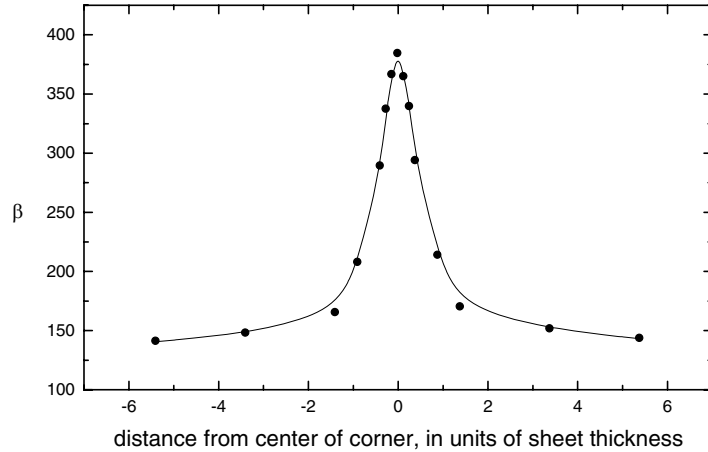


Fig. 2. Enhancement factor β on a line that runs along the tops of the rounded edges and traverses the corner, as a function of the distance from the center of the corner, for a sheet that has thickness 1 nm, height 500 nm and width 1000 nm.

Fig. 3(a) shows the dependence of β on $\cos(\theta)$, for some representative points on the surface of the corner. Similarly Fig. 3(b) shows the dependence of β on the transverse angle ϕ on the rounded edge, for a particular value of the distance d (in fact $t/4$) from the corner. The straight lines show linear fits (see below).

Finally, the values of β at the flat faces, far from the corner and edges, are small or zero and are therefore of no interest as field emission sources.

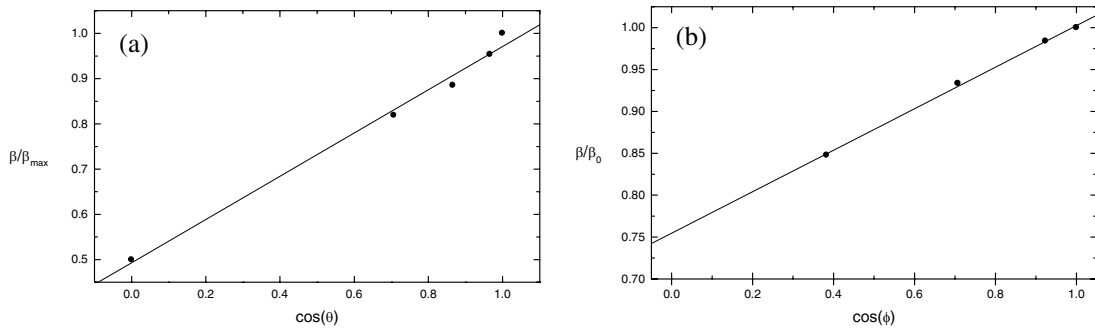


Fig. 3. Dependence of β on (a) the angle θ at the corner (see text) and (b) the transverse angle ϕ at the top edge in a plane $y = \text{constant}$.

3. Parameterization of field enhancement factors

The field enhancement factor β depends on the position on a corner or edge and it also depends on the dimensionless parameter h/t and to a lesser extent on h/w , where t , h and w are the thickness, height and width of the sheet respectively.

Starting with the maximum value of β , at the center of the corner, we find that the dependence on h/t of can be parameterized as:

$$\beta_{\max} = 2.16 \left(\frac{h}{t} \right)^{0.75} \quad (3)$$

The accuracy of this is approximately 5% for the range of h/t from 500 to 3000. The dependence of β_{\max} on h/w is much weaker and can be parameterized as:

$$\beta_{\max} \propto 1 + 0.09 \left(\frac{h}{w} \right) \quad (4)$$

Combining eqns (3) and (4) we obtain

$$\beta_{\max} = 2.07 \left(\frac{h}{t} \right)^{0.75} \left(1 + 0.09 \left(\frac{h}{w} \right) \right) \quad (5)$$

For the dependence shown in Fig. 2, along the tops of the rounded edges and traversing the corner, we find that the relative values β/β_{\max} are approximately independent of h/t or h/w . Therefore Fig. 2 can be used to obtain these relative values. Next we consider the parameterization of the dependence of β on the angle θ defined above for the corner. We find that

$$\frac{\beta}{\beta_{\max}} \approx (0.5 + 0.5 \cos \theta) \quad (6)$$

(in fact the coefficients for the line shown in Fig. 3(a) are 0.49 and 0.48 but for the present accuracy these can be replaced by those given in eqn. (6)). Combining eqns (5) and (6) we now obtain the overall parameterization for the surface of the corner:

$$\beta_{\text{corner}} = 2.07 \left(\frac{h}{t} \right)^{0.75} \left(1 + 0.09 \left(\frac{h}{w} \right) \right) (0.5 + 0.5 \cos \theta) \quad (7)$$

Finally we consider the edge. Along the top of the edge we find that β is approximately proportional to $(d/t)^{-0.19}$, where d is the distance from the junction of the edge and the corner. The value of β at the junction point (where $\theta = \pi/4$ and where the distance from the mid-point of the corner is $0.39t$) can be deduced from eqn (6) and is $0.854\beta_{\max}$. Therefore along the top of the edge:

$$\beta(d) = 0.85\beta_{\max} \left(\frac{d}{t} \right)^{-0.19} \quad (8)$$

The dependence on the transverse angle φ is found to be

$$\frac{\beta}{\beta_0} \approx (0.75 + 0.25 \cos \varphi) \quad (9)$$

where β_0 is the relevant value of $\beta(d)$ (in fact the coefficients for the line shown in Fig. 3(b) are 0.755 and 0.248). The overall parameterization for the surface of the edge is therefore:

$$\beta_{edge} = 1.77 \left(\frac{h}{t} \right)^{0.75} \left(1 + 0.09 \left(\frac{h}{w} \right) \right) (0.75 + 0.25 \cos \varphi) \left(\frac{d}{t} \right)^{-0.19} \quad (10)$$

Eqns (7) and (10) provide a complete parameterization of the parts of the sheet that are likely to be important for field emission.

4. Field emission current and curved sheets

To obtain the total field emission current from a graphene sheet it is necessary to integrate over the current density on all parts of the edge. The greatest contributions are expected to come from the corners, but the top ridge might also contribute significantly because although β is smaller there the area is much larger than the area of the corners. This will be the subject of a future publication. Methods of deducing the effective value of β from measured field-emission currents will also be discussed.

It is known that the graphite sheets are sometimes curved and not flat. The influence of this will also be the subject of a future publication.

Acknowledgements

SW and RSR gratefully acknowledge the NASA University Research, Engineering and Technology Institute on Bio Inspired Materials (BIMat; No. NCC-1-02037) and the National Science Foundation (No. 1421-M3/ CMS-0304506). SW appreciates the support of the Thai Ministry of Science and Technology on the Thai Government scholarship.

References

- [1] N. de Jonge and J-M. Bonard, Carbon Nanotube electron sources and applications. *Phil. Trans. R. Soc. Lond. A* 362 (2004) 2239-66.
- [2] Y. Saito, K. Hamaguchi, T. Nishino, K. Hata and K. Tohji, *Jpn. J. Appl. Phys., Part 2* 36 (1997) L1340.
- [3] J-M. Bonard, J-p. Salvetat, T. Stockli, L. Forro and A. Chatelain, *Appl. Phys. A* 69 (1999) 245.
- [4] Z.W. Pan, F.C.K. Au, H.L. Lai, W.Y. Zhou, L.F. Sun, Z.Q.Liu, D.S.Tang, C.S. Lee, S.T. Lee and S.S. Xie, *J. Phys. Chem. B* 105 (2001) 1519.
- [5] C. J. Edgcombe and U. Valdre, *Solid State Electron.* 45 (2001) 857.
- [6] C. J. Edgcombe and U. Valdre, *J. Microscopy* 203 (2001) 188.
- [7] V. Filip, D. Nicolaescu, F. Okuyama, *J. Vac. Sci. Technol. B* 19 (2001) 1016.
- [8] J.G. Leopold, O. Zik, E. Cheifetz and D. Rosenblatt, *J. Vac. Sci. Technol A* 19 (2001) 1790.
- [9] Ch. Adessi and M. Devel, *Phys. Rev. B* 65 (2002) 075418.
- [10] G. C. Kokkorakis, S. Modinos and J. P. Xanthakis, *J. Appl. Phys.* 91 (2002) 4580.
- [11] F.H. Read and N.J. Bowring, *Nuclear Instruments and Methods in Physics Research Section A.* 519 (2004) 305-314.
- [12] L. Nilsson, O. Groening, C. Emmenegger, O. Kuettel, E. Schaller, L. Schlapbach, H. Kind, J-M. Bonard and K. Kern, *Appl. Phys. Lett.* 76 (2000) 2071.
- [13] O. Gröning, O. M. Küttel, Ch. Emmenegger, P. Gröning and L. Schlapbach, *J. Vac. Sci. Technol. B* 18 (20001) 665.
- [14] A. Cao, X. Zhang, C. Xu, J. Liang, D. Wu and B. Wei, *Appl. Phys. A* 74 (2002) 415.
- [15] A.L. Musatov, N.A. Kiselev, D.N. Zakharov, E.F. Kukovitskii, A.I. Zhbanov, K.R. Izrael'yants and E.G. Chirkova, *Appl. Surf. Sc.* 183 (2001) 111.
- [16] V. Filip, D. Nicolaescu, M. Tanemura and F. Okuyama, *Ultramicroscopy* 89 (2001) 39.
- [17] F.H. Read and N.J. Bowring, *Microelectronic Engineering* 73-74 (2004) 679-685.
- [18] J. J. Wang, M. Y. Zhu, R. A. Outlaw, X. Zhao, D. M. Manos, B. C. Holloway, and V. P. Mammana, *Appl. Phys. Lett.*, 85 (2004) 1265-7.
- [19] CPO programs, available from www.electronoptics.com.
- [20] F H Read, *J. Computational Physics* 133 (1997) 1-5.
- [21] F. H. Read, *COMPEL* 23 (2004) 572-578.